ISSN: 2447-3359

REVISTA DE GEOCIÊNCIAS DO NORDESTE

Northeast Geosciences Journal

v. 11, nº 1 (2025)

https://doi.org/10.21680/2447-3359.2025v11n1ID37895

Incidence of Fatal yellowing of oil palm in response to soil penetration resistance

Incidência do Amarelecimento fatal da palma de óleo em resposta à resistência a penetração do solo

Nelson Ken Narusawa Nakakoji[1]; Ítala Duam Souza Narusawa[2]; Cleison Freitas da Silva[3]; Pedro Guerreiro Martorano[4]; Felix Lelis da Silva[5]; Paulo Roberto Silva Farias[6]; Tiago de Melo Sales[7]; Jose Gilberto Sousa Medeiros[8]; Javier Dias Pita[9]

[1] Universidade Federal Rural da Amazônia, PGAgro/UFRA, Belém/PA, Brasil. Email: narusawanelsonken@gmail.com
ORCID: https://orcid.org/0000-0001-7044-7877

[2] Universidade Federal do Rio Grande do Sul, PPGSR/CEPSRM, Porto Alegre/RS. Email: itala.narusawa@ufrgs.br
ORCID: https://orcid.org/0000-0002-6866-0959

[3] Instituto Federal de Educação, Ciência e Tecnologia do Pará, Castanhal/PA, Brasil. Email: eng.cleison@outlook.com
ORCID: https://orcid.org/0009-0003-0966-3943

[4] Universidade Federal Rural da Amazônia, PGAgro/UFRA, Belém/PA, Brasil. Email: pmartorano60@gmail.com
ORCID: https://orcid.org/0009-0005-8607-4776

[5] Instituto Federal de Educação, Ciência e Tecnologia do Pará, IFPA/Campus Castanhal/PA, Brasil. Email: felix.lelis@ifpa.edu.br
ORCID: https://orcid.org/0000-0001-8405-103X

[6] Universidade Federal Rural da Amazônia, UFRA/ Campus Belém/PA, Brasil. Email: paulorsfarias4@gmail.com
ORCID: https://orcid.org/0000-0001-9212-8957

[7] Instituto Federal de Educação, Ciência e Tecnologia do Pará, IFPA/Campus Castanhal/PA, Brasil. Email: tiago.sales@ifpa.edu.br
ORCID: https://orcid.org/0000-0002-4923-0881

[8] Instituto Federal de Educação, Ciência e Tecnologia do Pará, IFPA/Campus Castanhal/PA, Brasil. Email: gil.medeiros@ifpa.edu.br
ORCID: https://orcid.org/0000-0002-3287-4189

[9] Instituto Federal de Educação, Ciência e Tecnologia do Pará, IFPA/Campus Castanhal/PA, Brasil. Email: javier.pita@ifpa.edu.br
ORCID: https://orcid.org/0000-0002-8832-8005

Abstract: Studies on abiotic factors have gained increasing attention in research on Fatal Yellowing (FY) of oil palm (*Elaeis guineensis* Jacq.). The application of geostatistical techniques, especially ordinary kriging, enhances the analysis of these factors, providing a more holistic view of the study environment. This study aimed to analyze the influence of Soil Penetration Resistance (SPR) on the incidence of FY in oil palm, using geostatistical techniques. The study was conducted at Nogami Farm, in Igarapé-Açu (Pará State), in a 6.3-hectare oil palm plantation with 10.24% of affected plants. After measuring the SPR using a soil penetrometer, the data were subjected to descriptive and normality tests, followed by the construction of the semivariogram and the application of ordinary kriging, generating the thematic map of the spatial distribution of SPR. Based on the georeferenced phytosanitary inventory and the map, the SPR for each plant was determined, forming two groups: Plants with FY and Plants without FY. Given the non-normality of the data (Shapiro-Wilk test), the Mann-Whitney test was used, revealing a higher prevalence of FY in areas with higher SPR.

Keywords: Geostatistics; *Elaeis guineensis* Jacq.; Phytosanitary.

Resumo: Estudos sobre fatores abióticos têm ganhado destaque nas pesquisas sobre o Amarelecimento Fatal (AF) da palma-de-óleo (*Elaeis guineensis* Jacq.). A aplicação de técnicas geoestatísticas, especialmente a krigagem ordinária, amplia a análise desses fatores, proporcionando uma visão mais holística do ambiente de estudo. O presente trabalho objetivou analisar a influência da Resistência à Penetração do Solo (RPS) sobre a incidência do AF da palma-de-óleo, utilizando técnicas geoestatísticas. O estudo foi realizado na Fazenda Nogami, em Igarapé-Açu (Pará), em uma plantação de 6,3 hectares com 10,24% de plantas afetadas. Após aferir a RPS com um penetrômetro de solos, os dados foram submetidos a testes descritivos e de normalidade, seguidos pela construção do semivariograma e pela krigagem ordinária, gerando o mapa temático da distribuição espacial da RPS. A partir do inventário fitossanitário georreferenciado e do mapa, determinou-se a RPS para cada planta, constituindo dois grupos: Plantas Com AF e Plantas Sem AF. Dada a não normalidade dos dados (teste de Shapiro-Wilk), utilizou-se o teste de Mann-Whitney, revelando maior prevalência de AF em áreas com maior RPS.

Palavras-chave: Geoestatística; *Elaeis guineenses* Jacq.; Fitossanidade.

Received: 06/10/2024; Accepted: 07/03/2025; Published: 24/03/2025.

1. Introduction

Oil palm (*Elaeis guineensis* Jacq.) is one of the most productive palm species in terms of vegetable oil production, being widely cultivated in tropical regions. In recent decades, the expansion of this crop has been particularly notable in Southeast Asia, especially in Indonesia and Malaysia, the world's leading exporters of palm oil (SHAHBANDEH, 2024; TAN et al., 2022; LUKE et al., 2020; SAID et al., 2021). Colombia is the fourth-largest global producer, while Brazil ranks ninth, with the highest production concentrated in the state of Pará (FERNANDES et al., 2022; BENEZOLI et al., 2021; ABRAPALMA, 2024).

However, oil palm cultivation in Pará faces challenges with Fatal Yellowing (FY), a disease that affects oil palm and whose cause remains unknown. The first cases were reported in 1974, and since then, the disease has caused significant losses in cultivated areas in Pará, in addition to being recorded in other Latin American countries (GOMES JUNIOR et al., 2010; TORRES et al., 2016). The main symptom is root rot, which precedes leaf yellowing and, eventually, plant death (BOARI, 2008; GLORIA et al., 2021).

Studies indicate that abiotic factors, such as soil hypoxia, may be related to disease incidence, suggesting that nutrient deficiencies or inadequate management practices are potential factors (NASCIMENTO et al., 2018; TEIXEIRA et al., 2017; RODRIGUES-NETO et al., 2018). Soil penetration resistance (SPR) has been considered an important property for assessing soil compaction levels and its relationship with FY incidence (COLOMBI et al., 2018; MORAES et al., 2020).

In this scenario, the use of geostatistical methods, such as ordinary kriging, may play a key role in researching the relationship between SPR and FY incidence. This method allows the spatial prediction of attributes, facilitating the development of detailed maps of specific areas even with a limited number of samples (MOLIN; AMARAL; COLAÇO, 2015; YAMAMOTO, 2020; YAMAMOTO; LANDIM, 2013). This approach enhances the analysis of the variable, providing a broader understanding of the disease's responses concerning this soil characteristic.

Thus, given the economic importance of oil palm cultivation in Pará, the impact of FY on oil palm plantations, the soil-related factors as a likely cause of disease incidence, and the contribution of geostatistical methods to expand the analysis of SPR, this study aimed to evaluate the incidence of Fatal Yellowing (FY) in oil palm in response to soil penetration resistance (SPR).

2. Methodology

2.1 Study Area

The study was conducted at Nogami Farm, located in the municipality of Igarapé-Açu, in the northeastern mesoregion, Bragantina microregion, state of Pará, Brazil (IBGE, 2022), at UTM coordinates (Universal Transverse Mercator) zone 23 M: 9866989.65 and 9866783.58 south, 204042.58 and 204598.65 west (Figure 1).

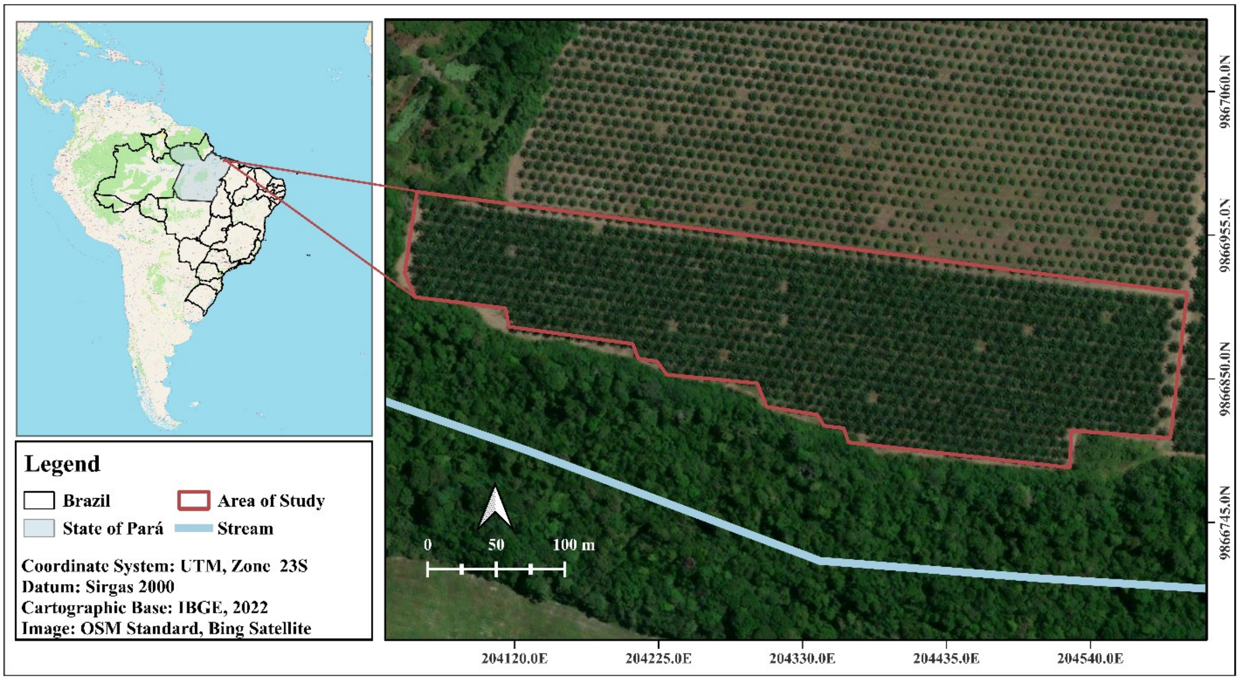

Figure 1 – Map of the Study Area Location.
Source: Authors (2024).

The climate of the region is classified as Ami according to the Köppen classification, corresponding to the super humid category. The annual minimum and maximum temperatures range from 21.7 to 32.2 °C, while the annual rainfall varies between 2,302.5 and 2,857.4 mm, with the highest precipitation occurring between March and April (PACHÊCO; BASTOS, 2007). The predominant soil in the area is Red-Yellow Latosol, which is suitable for agriculture (EMBRAPA, 2016). The 6.3 ha area was planted with *Elaeis guineensis* var. Tenera in 2010, using an equilateral triangle spacing of 8.5 m. Previously, the area was used as pasture for cattle. Annual fertilization is carried out based on the financial return of the crop, ranging from 1 to 5 kg per plant of synthetic fertilizer (NPK). Mowing is performed every 3 to 4 months. Both mowing and fruit bunch transport are conducted using heavy agricultural machinery.

2.2 Soil Penetration Resistance Survey (SPR)

The SPR data collection was carried out in April 2021. Sampling was conducted using a regular grid of 20 m × 20 m, resulting in 179 sampling points. To locate the sampling points, a Garmin 64s GNSS (Global Navigation Satellite System) navigation device was used. As a procedure, at each grid sampling point, the arithmetic mean of five sub-sample measurements taken within a 5 m radius of the grid point was calculated (Figure 2). This sampling method helps to reduce positioning errors and sampling errors of the studied variable (MOLIN; AMARAL; COLAÇO, 2015).

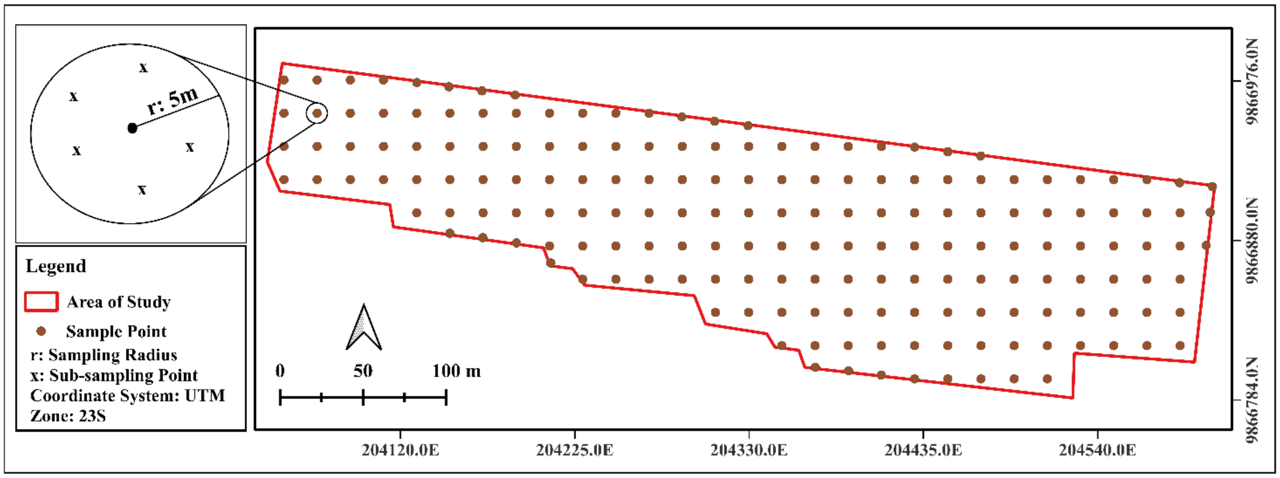

Figure 2 – Soil Penetration Resistance (SPR) Sampling Grid.
Source: Authors (2024).

The depth analysis was limited to 0–10 cm due to the interweaving of oil palm roots. Measurements were taken under dry conditions and at least six hours after any precipitation to avoid soil saturation. A single operator used a SOLO TEST penetrometer (REF. 1.210.001) to ensure consistency. After tabulating the collected data, the values were divided by 6.33 to obtain the metric in kgf/cm². The data were then converted to Megapascal (MPa) using the following conversion equation:

$$\text{RPS (MPa)} = 0.0980665^{*} \text{ x kgf/cm}^2 \quad (1)$$

Where:
* Conversion factor multiplier.

2.3 Survey of Fatal Yellowing of Oil Palm (FY)

The phytosanitary team of Nogami Farm identified the plants affected by Fatal Yellowing (FY) based on the symptomatology described by Boari (2008). A phytosanitary inventory was created in the second half of 2020. Initially, the data were recorded in row and plant coordinates and later converted to UTM coordinates using QGIS 3.34. The plants were georeferenced and classified in a shapefile as "Plants WITH FY" and "Plants WITHOUT FY," totaling 928 plants, of which 95 were diseased and 833 were healthy (Figure 3).

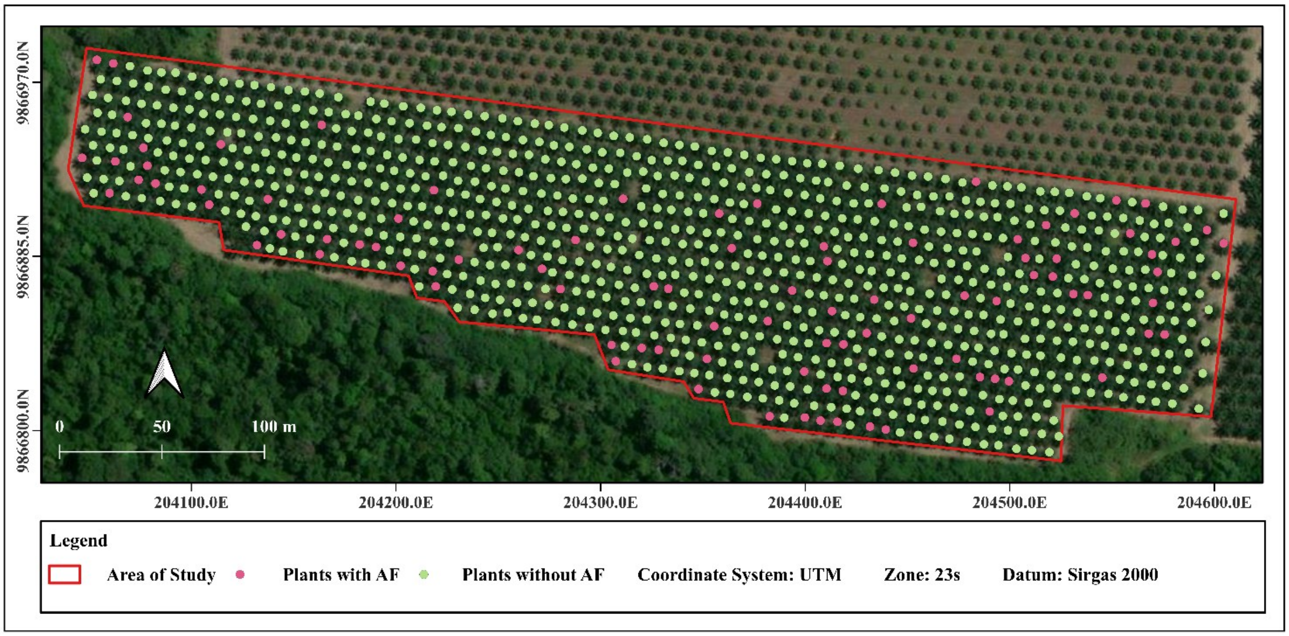

Figure 3 – Map of Fatal Yellowing of Oil palm incidence.
Source: Authors (2024).

2.4 Exploratory Data Analysis

After the field measurements and the conversion of SPR data to MPa, histograms and boxplots were generated, and the Shapiro-Wilk normality test was performed at a 5% significance level. Subsequently, a descriptive statistical analysis of the data was conducted, including the calculation of the mean, median, minimum, maximum, skewness, kurtosis, and coefficient of variation. These steps are essential for understanding the nature of the data, as they provide crucial information that aids in decision-making during the modeling process of the Experimental Semivariogram (ISAAKS; SRIVASTAVA, 1989; MOLIN; AMARAL; COLAÇO, 2015; YAMAMOTO, 2020).

2.5 Creation of the SPR Prediction Map

For the construction of the SPR prediction map, the geostatistical interpolation method of ordinary kriging was used. Initially, this method involves the development of the experimental semivariogram. The mathematical equation used to calculate the experimental semivariogram, according to Farias et al. (2002), is:

$$y(h) = \frac{1}{2n(h)} \sum_{i=1}^{n(h)} [Z(x_i + h) - Z(x_i)]^2 \quad (2)$$

Where:
$y(h)$= estimated semivariance at a distance interval (h)
$n(h)$ = number of sample pairs at a distance interval (h)
$Z(x_i)$, $Z(x_i + h)$= number of samples at two points separated by a distance interval (h)

After adjusting the parameters of the experimental semivariograms, the most suitable semivariogram model was selected to estimate the SPR semivariance. For this purpose, the spherical (3), exponential (4), and Gaussian (5) models were tested, as these are the most appropriate for soil science (DE OLIVEIRA; GREGO; BRANDÃO, 2015). According to Isaaks and Srivastava (1989), the three models are described as follows:

$$Esf(h) = C_0 + C_1[1{,}5(\frac{h}{a}) - 0{,}5(\frac{h}{a})^3] \quad For\ h < a$$
$$Esf(h) = C_0 + C_1 \quad For\ h \geq a \tag{3}$$

$$Exp(h) = C_0 + C_1[1 - \exp(-\frac{h}{a})] \tag{4}$$

$$Gau(h) = C_0 + C_1[1 - \exp(-\frac{h^2}{a^2})] \tag{5}$$

Where (for the three models):
C_0 = nugget effect
C_1 = partial sill
a = range
h = distance between the known point and the point to be estimated

To evaluate the quality of the semivariogram models in relation to the experimental SPR semivariogram, two indicators were analyzed: the coefficient of determination (R^2) and the root mean square error (RMSE). The closer R^2 is to 1 and RMSE is to 0, the better the fit of the semivariogram model to the experimental semivariogram (BHUNIA; SHIT; CHATTOPADHYAY, 2018; DE OLIVEIRA; GREGO; BRANDÃO, 2015). Their mathematical expressions are as follows:

$$R^2 = 1 - \frac{SQ_{res}}{SQ_{tot}} \quad \begin{cases} SQ_{res} = \sum_{i=1}^{n}(y_i - \hat{y}_i)^2 \\ SQ_{tot} = \sum_{i=1}^{n}(y_i - \bar{y}_i)^2 \end{cases} \tag{6}$$

$$RMSE = \sqrt{\frac{1}{n}\sum_{i=1}^{n}(y_i - \hat{y}_i)^2} \tag{7}$$

Where:
n = number of observations
y_i = fitted value of the experimental semivariogram
$\hat{y}_i$ = value estimated by the semivariogram model
$\bar{y}_i$ = mean of the fitted values of the experimental semivariograma

Another evaluation criterion was the Spatial Dependence Index (SDI), as suggested by Trangmar et al. (1986) and categorized by Cambardella et al. (1994), which aims to classify the proportion of variability resulting from spatial dependence into strong, moderate, and weak categories. The SDI is described by the following expression:

$$\text{IDE} = (\frac{C_0}{C_0 + C_1})100 \quad \begin{cases} \text{SDI} \leq 25, Strong \\ 25 < \text{SDI} < 75, Moderate \\ \text{SDI} \geq 75, Weak \end{cases} \tag{8}$$

Where:
C_0 = nugget effect
C_1 = partial sill

As a decisive test to determine the most suitable model among the semivariogram models with similar evaluation criteria, Cross-Validation (CV) was performed. This computational test consists of omitting one point from the sampling grid and predicting its value using ordinary kriging interpolation with the remaining points (YAMAMOTO, 2020). This process is repeated until all points have gone through the omission and prediction cycle. Thus, each model subjected to CV generates estimated and observed values. Consequently, the coefficient of determination (R^2_{cv}) and the root mean square error ($RMSE_{cv}$) can be calculated for each tested model. The closer the coefficient of determination is to 1 and the RMSE to 0, the better the semivariogram model fits the spatial variability of the SPR data collected in the field. Their mathematical equations are as follows:

$$R^2{}_{CV} = 1 - \frac{SQ_{res}}{SQ_{tot}} \quad \begin{cases} SQ_{res} = \sum_{i=1}^{n}(e_i - \hat{e}_i)^2 \\ SQ_{tot} = \sum_{i=1}^{n}(e_i - \bar{e}_i)^2 \end{cases} \tag{9}$$

$$\{RMSE_{CV} = \sqrt{\frac{1}{n}\sum_{i=1}^{n}(e_i - \hat{e}_i)^2} \tag{10}$$

Where
n = number of observations
ei = value observed at the point
$\hat{e}i$ = value estimated at the point through interpolation by ordinary kriging, using the semivariographic model
$\bar{e}i$ = average of the values observed at the points.After validating the semivariogram model that best represents the SPR, ordinary kriging interpolation was performed. This geostatistical interpolator allows estimating values of spatially distributed variables by using the structural properties of the semivariogram model (Nugget Effect, Sill, and Range), thus obtaining a covariance matrix between neighboring points and the point to be estimated. After this step, using the Lagrangian technique, the inverse matrix was calculated to obtain the weights of the SPR samples, whose sum was equal to 1 (YAMAMOTO; LANDIM, 2013). Subsequently, the ordinary kriging mathematical formula was applied to construct the prediction map:

$$z(x_0) = \sum_{i=1}^{n} \lambda_1 Z[x_1] \tag{11}$$

Where:
n = number of measured neighbors
$Z[x_1]$ = known value of each point
λ_1 = weights applied to each $Z[x_1]$

2.6 Data Extraction and Comparative Analysis

After generating the SPR prediction map, the "Sample Raster Values" tool in QGIS 3.34 was used in conjunction with the shapefile of the phytosanitary inventory of the study area to extract SPR values for each plant. This process allowed the creation of two independent groups ("Plants WITH FY" and "Plants WITHOUT FY") for comparative analysis.

Since the data from each group did not meet parametric assumptions, the non-parametric Mann-Whitney test was applied at a 5% significance level. Additionally, a boxplot was generated, and the medians of each group were calculated for a comparative demonstration of the data.

2.7 Software Used

For study replicability, this research exclusively used free and open-source software. The operating system employed was Linux Mint Debian Edition 6 Faye. Data organization and tabulation were performed using LibreOffice Calc. Statistical, geostatistical, and graphical analyses were conducted using the R programming language (version 4.2.2) (R CORE TEAM, 2022), combined with the RStudio graphical interface and the gstat, rstatix, psych, and ggplot2 packages.

For map layouts, the creation of the location map, and the phytosanitary map of FY, the open-source software QGIS 3.34 and the QuickMapServices plugin were used.

3. Results

3.1 Descriptive Statistics

The results of the descriptive statistical analysis of the field observations of SPR reveal a coefficient of variation of 19.47%, indicating low spatial variability. Additionally, negative skewness and kurtosis were observed, although both values were greater than -1. This suggests that the data are slightly concentrated to the right of the observer, with a mildly flattened curve. Despite the presence of asymmetric distributions in the data, the mean and median values are close, confirming that there is no pronounced skewness (Table 1).

Table 1 – Descriptive statistics of the SPR data analyzed at the depth of 0-10 cm.

Variable	Informations	Data
Soil Penetration Resistance (MPa)	Observations (n)	179
	Mean ($\bar{x}$)	3.03
	Median (M_d)	3.04
	Standard deviation (s)	0.59
	Variance (s^2)	0.35
	Minimum value	1.7
	Maximum value	4.28
	Coefficient of Skewness (Cs)	-0.16
	Coefficient of Kurtosis (Ck)	-0.57
	Coefficient of Variation (CV)	19.47%

Source: Authors (2024).

By analyzing the histogram, boxplot, and the results of the Shapiro-Wilk test, it can be concluded that the SPR data do not contain extreme values and exhibit a normal distribution (Figure 4). This characteristic, corroborated by descriptive statistics, reflects a good sampling density, which allowed for the effective capture of the spatial variability signature of the phenomenon. Consequently, this facilitates the process of adjusting the experimental semivariogram. However, it is important to emphasize that the normality condition of the data is not strictly required for the application of geostatistics and ordinary kriging.

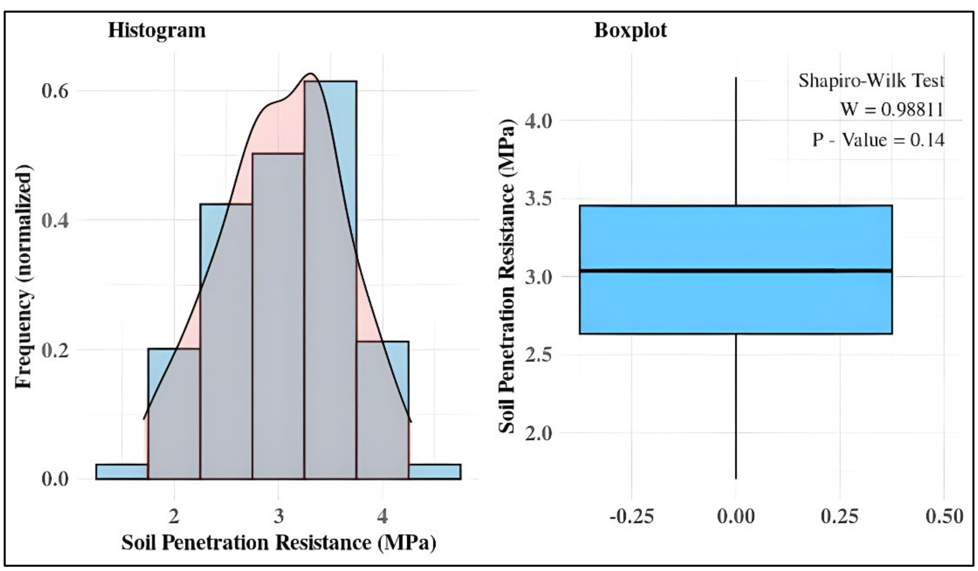

Figure 4 – Histogram, Bosplot and Shapiro Wilk Test data analyzed at the 0-10 cm depth.
Source: Authors (2024).

3.2 Geostatistical Analysis

Considering the measurements of Soil Penetration Resistance (SPR), the geostatistical analyses performed, and the cross-validation procedures applied, it was possible to adjust the experimental semivariogram, with the variable's behavior best represented by the Exponential model (Figure 5).

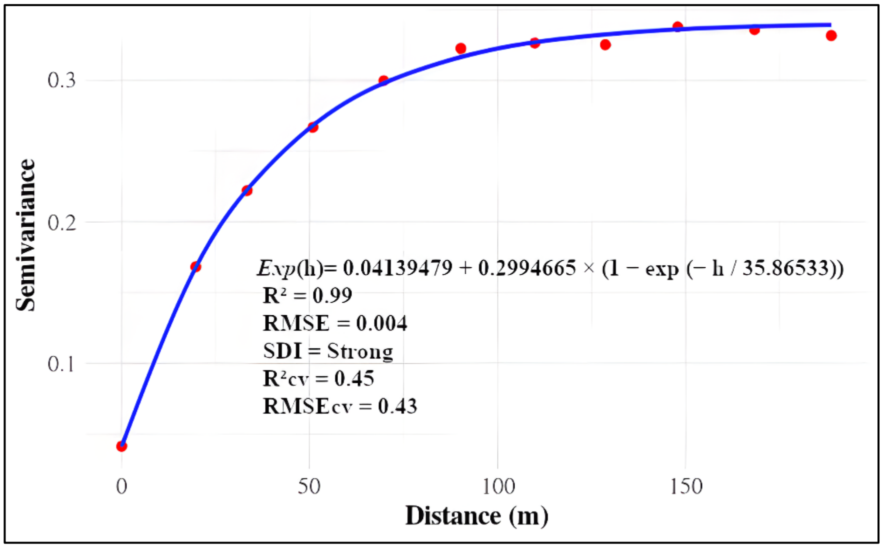

Figure 5 – Adjustment of the semivariogram model and its parameters for SPR analyzed at the depth of 0-10 cm. Source: Authors (2024).

The coefficient of determination (R^2) showed a significant proximity to 1, indicating a strong fit of the model to the experimental semivariogram. Additionally, the root mean square error (RMSE) approached zero, suggesting a good predictive capability of the model. The Spatial Dependence Index (SDI) revealed a strong spatial correlation between observations, with the model's range estimated at 35.87 meters — a relatively low value — indicating frequent variations in Soil Penetration Resistance (SPR) over short distances. The R^2_{cv} and $RMSE_{cv}$ values stood out as the most favorable among the three evaluated models, confirming the exponential model as the most suitable among the tested models.

3.3 Oil Plam FY incidence in response to SPR

By analyzing the spatial distribution of FY incidence and the spatial variability of SPR, which ranged from 1.88 to 4.05 MPa, it is demonstrated that their concentrations are more pronounced in the southern part of the study area, indicating an influence of SPR on disease incidence (Figure 6).

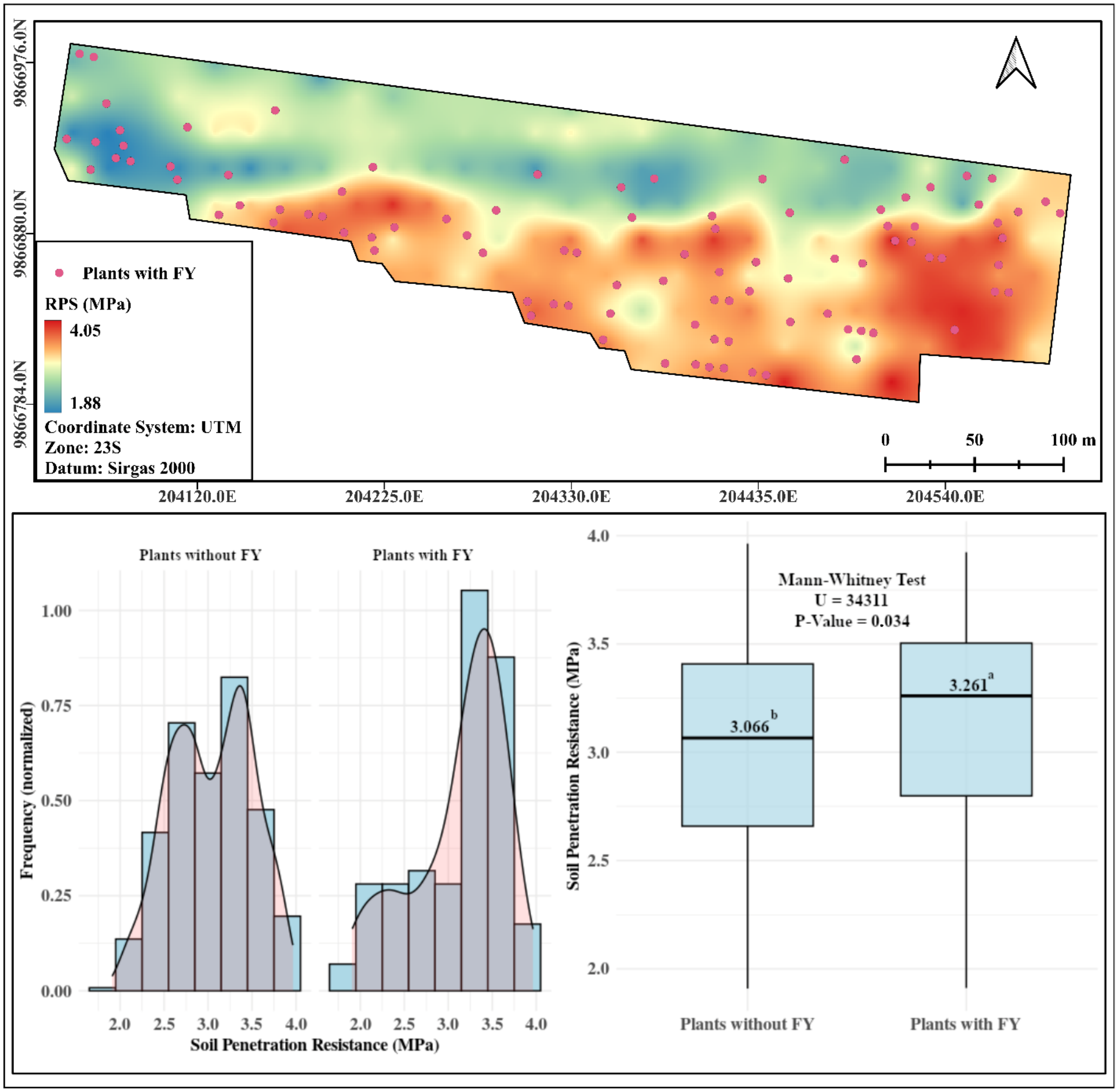

Figure 6 – Prediction map of SPR, Spatial distribution of FY Histogram, and Boxplot of SPR for Plants with FY and Plants without FY groups.
Source: Authors (2024).

This finding is corroborated by the analysis of the histograms for the groups "plants with FY" and "plants without FY," which reveal a higher concentration of diseased plants in areas where SPR values are more pronounced. This is evidenced by the central tendency of the histogram for "plants with FY," which is shifted to the right, around 3.5 MPa.

Additionally, the boxplot analysis shows a higher median for the "plants with FY" group, indicating statistically significant differences between the groups, as confirmed by the Mann-Whitney test at a 5% significance level. Therefore, these data suggest that areas with higher SPR values exhibit a greater incidence of FY in oil palm.

4. Discussion

The descriptive analysis phase is extremely important in data analysis, as it allows for the identification of errors, ranging from data output failures to calibration errors in the equipment, and provides a preliminary understanding of the behavior of the studied variable (AMARAL; FIGUEIREDO, 2022; MOLIN; AMARAL; COLAÇO, 2015).

Another important factor is the coefficient of variation (CV). According to the principles outlined by Pimentel-Gomes (2022) in the context of classical statistics, measuring the coefficient of variation is a fundamental indicator in field experimental settings. From this perspective, a coefficient of variation below 10% indicates high precision, reflecting the methodological consistency of the study. Additionally, values between 10% and 20% are considered good, maintaining a satisfactory level of precision.

However, according to the same author, when the coefficient exceeds the 20%–30% range, it indicates increasing uncertainty, which compromises the reliability of the results. Above 30%, the coefficient of variation denotes excessive variability, undermining the experiment's conclusions. In this context, detecting a coefficient of variation below 20% in the SPR field measurements at the 0–10 cm layer reaffirms the good precision of the experiment, providing a reliable foundation for subsequent analyses.

Regarding geostatistical parameters, the reliability of the semivariogram model fit to the experimental semivariogram can be evaluated through the coefficient of determination (R^2), which was 0.99 for the exponential model of the SPR variable. As indicated by Tavanti et al. (2019), semivariogram models with R^2 values of 0.50 or higher already demonstrate an acceptable fit, reinforcing the robustness of the model used for SPR analysis.

Another analytical criterion is the range of the semivariogram model, which indicates the spatial dependence radius of the variable, that is, the extent to which values remain similar over distance (MOLIN; AMARAL; COLAÇO, 2015; YAMAMOTO, 2020; YAMAMOTO; LANDIM, 2013). In the study area, within the oil palm plantation, this range was determined to be 35.87 m for SPR. This variable is highly sensitive to the mechanical stress to which the soil is subjected (NEGRÓN; LÓPEZ; DÖRNER, 2019). Studies have shown that in areas such as pastures, which are subject to constant cattle trampling, SPR in the 0–10 cm soil layer increased by 800% over time, with range values varying between 8 and 12 m (BATISTA et al., 2024).

Meanwhile, in sugarcane plantations, where all operations, from planting to harvesting, are mechanized—a condition slightly less intense than in pastures—the range values varied between 22 and 24 m (SOUZA; MARQUES JÚNIOR; PEREIRA, 2004). This suggests that mechanical stress is less pronounced in oil palm cultivation compared to these agroecosystems, as some practices, such as pruning and harvesting (except for fruit bunch collection), are still performed manually. However, the range parameter alone does not necessarily indicate good soil conditions.

Regarding SPR, it is important to note that values between 2 and 4 MPa are considered high (BEUTLER et al., 2001; SILVA et al., 2020; VALADÃO et al., 2011), indicating an unfavorable condition in the study area, where values ranged from 1.88 to 4.05 MPa. In this context, intense traffic of heavy machinery emerges as the primary factor contributing to mechanical stress. Due to the lack of seasonality in production, oil palm harvesting occurs continuously throughout the year. During the rainy season, machinery operations for fruit bunch collection induce the formation of soil crusts, increasing particle cohesion and consequently leading to a significant rise in SPR (YU et al., 2024). More localized studies have demonstrated that SPR is more pronounced in the traffic lanes of agricultural implements than in areas designated exclusively for oil palm mulch deposition (SATO et al., 2017).

In the context of FY incidence, one of the potential causes is soil hypoxia. This condition promotes an increase in reduced ions such as Fe^{2+}, Mn^{3+} e NO^{3+} in the soil solution, leading to damage to the root system and subsequent manifestation of symptoms associated with FY (TEIXEIRA et al., 2017). In areas where SPR is higher, indicating greater compaction and lower soil aeration, there is a potential for an increased migration of these reduced ions into the soil solution. Additionally, soils with higher clay content tend to have metallic oxides in their mineralogy and greater cohesion between their particles, which contributes to higher SPR and a greater concentration of metallic oxides such as iron and manganese in the soil solution, thereby exacerbating plant intoxication (NASCIMENTO et al., 2018).

However, studies indicate that soils with higher biological activity exhibit a greater incidence of FY (NAKAKOJI, 2024). This biological activity can only be observed in soils predominantly under aerobic conditions, as it has been demonstrated that anaerobic activity, which solubilizes metallic ions, is considerably lower than aerobic activity (PRIMAVESI, 2022; SCHAEFER, 2012). Therefore, the biological activity levels found in this study suggest that soil hypoxia may not be the sole cause of FY, prompting the investigation of other factors such as plant malnutrition.

In soils with high SPR, root shortening occurs along with reduced air availability, leading to decreased cellular respiration in plants, making them more vulnerable to opportunistic microorganisms (JUNIOR et al., 2014; PRIMAVESI, 2022), particularly in areas where biological activity is more pronounced. These microorganisms can trigger the degradation of tender roots, which are responsible for water and nutrient absorption, ultimately leading to the characteristic symptoms of FY.

An additional analysis conducted to detect metabolites extracted from leaf samples of both healthy and diseased plants revealed a deficiency in nine metabolites in plants affected by FY, with two standing out in particular: tyramine and glycerophosphorylcholine (GPC) (RODRIGUES-NETO et al., 2018). Tyramine is recognized as a crucial metabolite used by plants in response to insect and herbivore attacks, as well as having defensive properties against salinity in rice crops. In Solanaceae species, tyramine is synthesized in response to pathogen-induced damage (GUILLET; DE LUCA, 2005; LEFÈVRE; GRATIA; LUTTS, 2001; SERVILLO et al., 2017).

Regarding GPC, during the catabolic process mediated by extracellular phosphodiesterases, choline is absorbed and distributed within plant cells, playing a fundamental role in lipid regulation (KHAN; FARIDUDDIN; YUSUF, 2017; VAN DER REST et al., 2002). The elevation of extracellular phosphodiesterase enzymes, commonly observed under phosphorus deficiency conditions, leads to a reduction in GPC levels (RODRIGUES-NETO et al., 2018), This deficiency, combined with the absence of tyramine, may increase the vulnerability of young oil palm roots, potentially triggering Fatal Yellowing Syndrome.

As a hypothesis, it is plausible to suggest that an increase in soil penetration resistance (SPR) may trigger a nutritional imbalance in oil palm, thereby contributing to the deficiency of the metabolites mentioned. This imbalance is further exacerbated by soil hypoxia, as previously mentioned, and by an increase in clay content—both phenomena that coincide with higher SPR values. An increase in the proportion of clay, in turn, promotes a rise in SPR and consequently facilitates the immobilization of phosphorus by metallic oxides present in the soil (DOS SANTOS et al., 2020), leading to GPC deficiency. This set of adverse conditions further worsens the plant's unfavorable state, contributing to the development of FY symptomatology.

It is also important to highlight the role of genetic factors in the manifestation of FY, as healthy and diseased plants often share the same environment, where they exhibit similar SPR characteristics. This observation may be related to the genetic variability inherent to the Tenera cultivar, which originates from heterogeneous populations (GOMES JR. et al., 2014). This genetic diversity provides the cultivar with a broad range of phenotypic expressions, such as variable trunk diameters, plant heights, and oil production, among other traits that are easily observed in the field.

Thus, it is plausible that within this genetic diversity, there are individuals that possess greater resistance to adverse soil conditions and, therefore, never exhibit FY symptomatology. This genetic adaptability may be a determining factor in the plants' ability to tolerate and recover from unfavorable soil conditions, emphasizing the importance of selecting more resistant specimens to ensure the productivity and sustainability of oil palm cultivation.

4. Final Considerations

The development of spatial variability maps of soil penetration resistance (SPR) is a valid and promising method, capable of identifying areas that require intervention to improve soil conditions and, consequently, mitigate the incidence of Fatal Yellowing (FY) in oil palm.

However, it is crucial to recognize that SPR alone does not fully explain the causes of this disease. There remains a significant need for further in-depth studies on edaphoclimatic and genetic factors to clarify the underlying causes of FY.

Acknowledgments

The authors thank the Federal Institute of Education, Science, and Technology of Pará (IFPA) for the technical support provided and for making the penetrometer available. With great appreciation, we also thank Nogami Farm for granting access to the study area and providing data on Fatal Yellowing (FY). Additionally, the first author extends sincere gratitude to the ecologist Dr. Maurício Humberto Vancine for his valuable contribution in providing configurations that enabled the adaptation of R for geoprocessing applications, significantly contributing to the development of this study.

References

ABRAPALMA – ASSOCIAÇÃO BRASILEIRA DE PRODUTORES DE ÓLEO DE PALMA. Diagnóstico da palma de óleo brasileira. Available at: http://www.abrapalma.org/pt/a-palma-no-brasil-e-no-mundo/. Accessed on: March 23, 2024.

AMARAL, L. R. DO; FIGUEIREDO, G. K. D. Geoprocessamento aplicado ao gerenciamento de lavouras. In: *Agricultura digital*, 2. ed. São Paulo, SP: Oficina de Textos, 2022.

BATISTA, P. H. D. et al. Assessment spatial soil physical properties under rotational cattle grazing in Northeastern Brazil. 2024.

BENEZOLI, V. H. et al. Modeling oil palm crop for Brazilian climate conditions. *Agricultural Systems*, v. 190, p. 103130, May 2021.

BEUTLER, A. N. et al. Resistência à penetração e permeabilidade de latossolo vermelho distrófico típico sob sistemas de manejo na região dos cerrados. *Revista Brasileira de Ciência do Solo*, v. 25, n. 1, p. 167–177, Mar. 2001.

BHUNIA, G. S.; SHIT, P. K.; CHATTOPADHYAY, R. Assessment of spatial variability of soil properties using geostatistical approach of lateritic soil (West Bengal, India). *Annals of Agrarian Science*, v. 16, n. 4, p. 436–443, Dec. 2018.

BOARI, A. DE J. Estudos realizados sobre o amarelecimento fatal do dendezeiro (*Elaeis guineensis* Jacq.) no Brasil. *Documentos 348*, n. 1ª ed., p. 66, 2008.

CAMBARDELLA, C. A. et al. Field-scale variability of soil properties in central Iowa soils. *Soil Science Society of America Journal*, v. 58, n. 5, p. 1501–1511, 1994.

COLOMBI, T. et al. Feedbacks between soil penetration resistance, root architecture and water uptake limit water accessibility and crop growth – A vicious circle. *Science of The Total Environment*, v. 626, p. 1026–1035, Jun. 01, 2018.

DE OLIVEIRA, R. P.; GREGO, C. R.; BRANDÃO, Z. N. Geoestatística aplicada na agricultura de precisão utilizando o Vesper. Brasília, DF: Embrapa, 2015.

DOS SANTOS, D. et al. Ciclo biogeoquímico do fósforo, diagnóstico de disponibilidade e adubação fosfatada. [s.l.: s.n.].

EMBRAPA – EMPRESA BRASILEIRA DE PESQUISA AGROPECUÁRIA. Mapas de solos e de aptidão agrícola das áreas alteradas do Pará. Available at: https://ainfo.cnptia.embrapa.br/digital/bitstream/item/147241/1/MapasSolosPara.pdf. Accessed on: March 23, 2024.

FARIAS, P. R. S. et al. Using geostatistical analysis to evaluate the presence of *Rotylenchulus reniformis* in cotton crops in Brazil: economic implications. *Journal of Nematology*, v. 34, n. 3, p. 232–238, Sep. 2002.

FERNANDES, J. A. F. et al. Contexto socioambiental del cultivo extensivo de palma en Colombia. *Mercator (Fortaleza)*, v. 21, p. e21007, May 18, 2022.

GLORIA, G. C. P. et al. Root morphological traits of oil palm genotypes with differential resistance to fatal yellowing. *Semina: Ciências Agrárias*, v. 42, n. 6, p. 3073–3088, Aug. 12, 2021.

GOMES JR., R. A. et al. Evaluation of interspecific hybrids of palm oil reveals great genetic variability and potential selection gain. *Industrial Crops and Products*, v. 52, p. 512–518, Jan. 01, 2014.

GOMES JUNIOR, R. A. et al. Bases técnicas para a cultura da palma de óleo integrado na unidade produtiva da agricultura familiar. Belém, PA: Embrapa Amazônia Oriental, 2010.

GUILLET, G.; DE LUCA, V. Wound-inducible biosynthesis of phytoalexin hydroxycinnamic acid amides of tyramine in tryptophan and tyrosine decarboxylase transgenic tobacco lines. *Plant Physiology*, v. 137, n. 2, p. 692–699, Feb. 01, 2005.

IBGE – INSTITUTO BRASILEIRO DE GEOGRAFIA E ESTATÍSTICA. IBGE | Cidades@ | Pará | Igarapé-Açu | Panorama. Available at: https://cidades.ibge.gov.br/brasil/pa/igarape-acu/panorama. Accessed on: March 24, 2024.

ISAAKS, E. H.; SRIVASTAVA, R. M. Applied geostatistics. New York: *Oxford University Press*, 1989.

JUNIOR, D. D. V. et al. Penetration resistance according to penetration rate, cone base size and different soil conditions. *Bragantia*, v. 73, p. 171–177, Jun. 2014.

KHAN, T. A.; FARIDUDDIN, Q.; YUSUF, M. Low-temperature stress: is phytohormones application a remedy? *Environmental Science and Pollution Research*, v. 24, n. 27, p. 21574–21590, Sep. 2017.

LEFÈVRE, I.; GRATIA, E.; LUTTS, S. Discrimination between the ionic and osmotic components of salt stress in relation to free polyamine level in rice (*Oryza sativa*). *Plant Science*, v. 161, n. 5, p. 943–952, Oct. 2001.

LUKE, S. H. et al. Managing oil palm plantations more sustainably: large-scale experiments within the biodiversity and ecosystem function in tropical agriculture (BEFTA) programme. *Frontiers in Forests and Global Change*, v. 2, Jan. 08, 2020.

MOLIN, J. P.; AMARAL, L. R. DO; COLAÇO, A. F. Agricultura de precisão. 1. ed. São Paulo, SP: *Oficina de Textos*, 2015.

MORAES, M. T. DE et al. Soil compaction impacts soybean root growth in an Oxisol from subtropical Brazil. *Soil and Tillage Research*, v. 200, p. 104611, Jun. 01, 2020.

NAKAKOJI, N. K. N. et al. Geo-statistical analysis of enzymatic, chemical, and granulometric soil attributes in response to the incidence of Fatal Yellowing in oil palm. Revista de Gestão Social e Ambiental, v. 18, n. 10, e08995, 2024. Available at: https://doi.org/10.24857/rgsa.v18n10-214. Accessed on: March 01, 2025.

NASCIMENTO, S. V. DO et al. Differential accumulation of proteins in oil palms affected by fatal yellowing disease. *PLOS ONE*, v. 13, n. 4, p. e0195538, April 05, 2018.

NEGRÓN, M.; LÓPEZ, I.; DÖRNER, J. Consequences of intensive grazing by dairy cows of contrasting live weights on volcanic ash topsoil structure and pasture dynamics. *Soil and Tillage Research*, v. 189, p. 88–97, Jun. 2019.

PACHÊCO, N. A.; BASTOS, T. X. Boletim Agrometeorológico 2006 - Igarapé-Açu. *Documentos 296*, p. 30, 2007.

PIMENTEL-GOMES, F. Curso de estatística experimental. 15. ed. Piracicaba, SP: Fealq, 2022.

PRIMAVESI, A. M. Manual do solo vivo. 2. ed. São Paulo, SP: *Expressão Popular*, 2022.

R CORE TEAM. R: A Language and Environment for Statistical Computing. R Foundation for Statistical Computing, Vienna, Austria. Available at: https://www.R-project.org/. Accessed on: Feb. 04, 2024.

RODRIGUES-NETO, J. C. et al. Metabolic fingerprinting analysis of oil palm reveals a set of differentially expressed metabolites in fatal yellowing symptomatic and non-symptomatic plants. *Metabolomics*, v. 14, n. 10, p. 142, Oct. 11, 2018.

SAID, F. F. et al. A probe into the status of the oil palm sector in the Malaysian value chain. *Economies*, v. 9, n. 3, p. 106, Sep. 2021.

SATO, M. K. et al. Least limiting water range for oil palm production in Amazon region, Brazil. *Scientia Agricola*, v. 74, n. 2, p. 148–156, April. 2017.

SCHAEFER, C. E. G. R. Pedologia: fundamentos. [s.l.]: Sbcs, 2012.

SERVILLO, L. et al. Tyramine pathways in citrus plant defense: glycoconjugates of tyramine and its N-methylated derivatives. *Journal of Agricultural and Food Chemistry*, v. 65, n. 4, p. 892–899, Feb. 01, 2017.

SHAHBANDEH, M. Vegetable oils consumption worldwide 2023/24. Available at: https://www.statista.com/statistics/263937/vegetable-oils-global-consumption/. Accessed on: March 23, 2024.

SILVA, G. J. et al. Resistência à penetração em solo sob pastagem degradada. *Cultura Agronômica: Revista de Ciências Agronômicas*, v. 29, n. 2, p. 256–273, July 13, 2020.

SOUZA, Z. M.; MARQUES JÚNIOR, J.; PEREIRA, G. T. Variabilidade espacial de atributos físicos do solo em diferentes formas do relevo sob cultivo de cana-de-açúcar. *Revista Brasileira de Ciência do Solo*, v. 28, n. 6, p. 937–944, Dec. 2004.

TAN, X. J. et al. Expert systems in oil palm precision agriculture: a decade systematic review. *Journal of King Saud University - Computer and Information Sciences*, v. 34, n. 4, p. 1569–1594, April 01, 2022.

TAVANTI, R. F. R. et al. Least limiting water as a soil indicator in an integrated crop-livestock systems of the Cerrado, Brazil. *Geoderma Regional*, v. 19, p. e00232, Nov. 2019.

TEIXEIRA, W. G. et al. A hipótese abiótica como agente causal do amarelecimento fatal (AF) da palma de óleo (*Elaeis guineensis* Jacq.) no Brasil. *Amazônia e seus solos: peculiaridades e potencialidades*. Anais... In: CONGRESSO BRASILEIRO DE CIÊNCIA DO SOLO, Belém, PA: SBCS, 2017.

TORRES, G. A. et al. Bud rot caused by *Phytophthora palmivora*: a destructive emerging disease of oil palm. *Phytopathology®*, v. 106, n. 4, p. 320–329, April. 2016.

TRANGMAR, B. B.; YOST, R. S.; UEHARA, G. Application of geostatistics to spatial studies of soil properties. In: ADVANCES IN AGRONOMY, Hawaii: Elsevier, 1986. v. 38, p. 45–94.

VALADÃO, F. C. D. A. et al. Variação nos atributos do solo em sistemas de manejo com adição de cama de frango. *Revista Brasileira de Ciência do Solo*, v. 35, n. 6, p. 2073–2082, Dec. 2011.

VAN DER REST, B. et al. Glycerophosphocholine metabolism in higher plant cells: evidence of a new glyceryl-phosphodiester phosphodiesterase. *Plant Physiology*, v. 130, n. 1, p. 244–255, Sep. 01, 2002.

YAMAMOTO, J. K. Estatística, análise e interpolação de dados geoespaciais. 1. ed. São Paulo: *Grafica Paulos*, 2020.

YAMAMOTO, J. K.; LANDIM, P. M. B. Geoestatística: conceitos e aplicações. São Paulo: *Oficina de Textos*, 2013.

YU, C. et al. The effects of soil compaction on wheat seedling root growth are specific to soil texture and soil moisture status. *Rhizosphere*, v. 29, p. 100838, Mar. 2024.